All-optical reshaping of light pulses by using $\chi^{(2)}$ media

Kuanshou Zhang,* Laurent Longchambon, Thomas Coudreau,† and Claude Fabre

Laboratoire Kastler Brossel, Université Pierre et Marie Curie, Campus Jussieu, Case 74, 75252 Paris Cedex 05, France

Received February 28, 2003; revised manuscript received May 9, 2003

We have developed a new method based on two cavities containing $\chi^{(2)}$ media to reshape optical pulses by an all-optical technique. The system is entirely passive; i.e., all the energy is brought by the incoming pulse and uses two successive optical cavities with independent thresholds. The output pulse is close to a rectangular shape. We show that this technique could be extended to high bit rates and telecommunication wavelength by using very small cavities containing current nonlinear materials. © 2003 Optical Society of America

OCIS codes: 190.4410, 190.4970, 320.5540.

1. INTRODUCTION

In optical telecommunications, multiple amplification and attenuation of information-carrying light pulses leads to an amplification of noise that quickly deteriorates the pulse shape and therefore increases the bit error rate. To overcome such a signal distortion, one can use an active technique of pulse regeneration, which is usually performed by optoelectronic techniques. The so-called 3R regeneration implies a reamplification, reshaping, and retiming of the pulses. An all-optical method to perform these different regeneration functions would be potentially faster and with broader bandwidths. Several methods, based on third-order nonlinearities or nonlinear amplifiers,[1,2] have been proposed so far and are actively being studied to implement this function.

Second-order nonlinearities have not so far been studied to implement regeneration functions, in spite of the high nonlinear effects that they are likely to produce even at low input powers and in spite of their intrinsic ultrashort response time. We propose here a passive and efficient method, which uses two successive optical cavities containing nonlinear $\chi^{(2)}$ crystals, for reshaping optical pulses. We give the results of a first experiment, which show that our proposed scheme is actually able to reshape low-power light pulses, performed at 1.06 μm and at low bit rates. We also discuss the potentialities of the extension of our technique to real optical telecommunication conditions.

Our scheme consists of two nonlinear optical cavities that have input–output characteristics with a threshold behavior and lead to a reshaping of the input pulse. The first cavity has a minimum threshold: As in a laser or an optical parametric oscillator (OPO), no significant power exits the cavity below a certain value, $P_{\text{threshold}}^{\text{low}}$ of the pump power. As a result, below $P_{\text{threshold}}^{\text{low}}$ the transmitted power is zero. The second cavity has a maximum threshold $P_{\text{threshold}}^{\text{high}}$: An input signal with a power above $P_{\text{threshold}}^{\text{high}}$ is transmitted with a constant value equal to $P_{\text{threshold}}^{\text{high}}$. The total transfer function of the two optical devices put in series is thus a steep Heaviside step function: With an incident distorted pulse, the output pulse is close to a square pulse.

We begin in Section 2 by giving the theoretical expressions of the transfer functions of the two cavities. Section 3 is devoted to the description of the experimental setup, and in Section 4 we describe the experimental results obtained at the wavelength of 1.06 μm. Finally, in Section 5 we analyze the possibility of applying these ideas to pulses having a wavelength of 1.5 μm and to very high bit rates.

2. THEORETICAL ANALYSIS

A. First Optical System: Intracavity Second-Harmonic Generation–Optical Parametric Oscillator

The first cavity contains a type-II $\chi^{(2)}$ crystal and is illuminated by a beam at frequency ω_0, polarized linearly at +45° of the crystal axes. The cavity is assumed to be resonant, at the same time, for the ordinary and extraordinary waves at the input frequency ω_0 and for its second harmonic $2\omega_0$ and to have a single coupling mirror at both frequencies. The following well-known equations[3] describe the nonlinear resonant coupling between the intracavity amplitudes of the three interacting fields in the steady-state regime and in the case of exact triple resonance:

$$(1 - r)A_1 = gA_0A_2^* + t\frac{1}{\sqrt{2}}A^{\text{in}}, \tag{1}$$

$$(1 - r)A_2 = gA_0A_1^* + t\frac{1}{\sqrt{2}}A^{\text{in}}, \tag{2}$$

$$(1 - r_0)A_0 = -gA_1A_2, \tag{3}$$

where A_1 and A_2 are the intracavity ordinary and extraordinary wave envelope amplitudes at the fundamental frequency ω_0, A_0 is the intracavity second-harmonic amplitude, A^{in} is the input field amplitude, r and t are the amplitude reflection and transmission coefficients of the

cavity's coupling mirror at the fundamental frequency, and r_0 and t_0 are the same quantities at the second-harmonic frequency. These equations can be simplified if one introduces the rotated basis,

$$A_{\pm} = \frac{1}{\sqrt{2}}(A_1 \pm A_2),$$

which represents the amplitude of the fundamental field along the two directions at $\pm 45°$ from the crystal's extraordinary and ordinary directions. The steady-state equations can now be written in a decoupled form:

$$(1 - r)A_+ = -gA_0A_+^* + tA_+^{\text{in}}, \tag{4}$$

$$(1 - r)A_- = +gA_0A_-^*, \tag{5}$$

$$(1 - r_0)A_0 = -\frac{g}{2}(A_+^2 - A_-^2). \tag{6}$$

These equations can be readily solved.[4] One finds that there are two different regimes, depending on the input intensity $P^{\text{in}} = |A^{\text{in}}|^2$, separated by a "pitchfork bifurcation" occurring at an intensity $P_{\text{threshold}}^{\text{low}}$ (Ref. 5) (see Fig. 1):

1. For $P^{\text{in}} < P_{\text{threshold}}^{\text{low}}$, one has

$$A_- = 0, \tag{7}$$

$$\left[1 - r - \frac{g^2}{2(1 - r_0)}|A_+|^2\right]A_+ = tA_+^{\text{in}}, \tag{8}$$

$$A_0 = -\frac{g}{2(1 - r_0)}A_+^2. \tag{9}$$

This is the usual behavior of an intracavity doubly resonant frequency doubler, in which more and more pump power is converted into the second harmonic as the pump power increases.

2. For $P^{\text{in}} > P_{\text{threshold}}^{\text{low}}$, one has $A_- \neq 0$ and

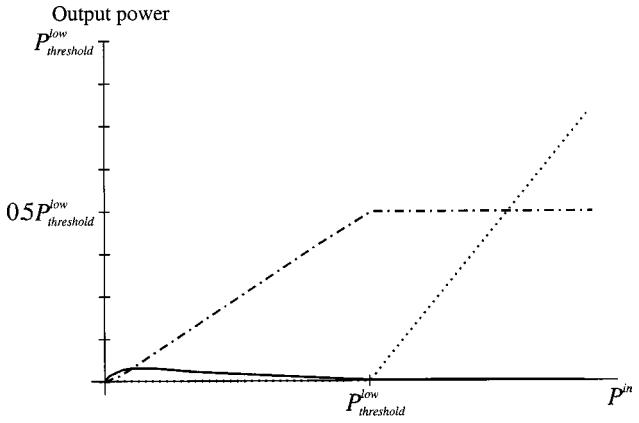

Fig. 1. Intracavity pump power along the + polarization, $|A_+|$ (solid curve), intracavity pump power along the − polarization, $|A_-|^2$ (dotted line), and intracavity second-harmonic power, $|A_0|^2$ (dashed–dotted curve), for the first cavity as a function of the input pump power.

$$A_+ = \frac{t}{2(1 - r)}A_+^{\text{in}}, \tag{10}$$

$$A_-^2 = \frac{1 + r}{4(1 - r)}(A_+^{\text{in}})^2 - \frac{2(1 - r)(1 - r_0)}{g^2}, \tag{11}$$

$$A_0 = \frac{1 - r}{g}. \tag{12}$$

The intracavity second-harmonic power is sufficient to generate an oscillation on the A_- mode. The behavior of the system is similar to an OPO: The second-harmonic field is now clamped to its threshold value while the A_- power increases linearly with the input power. If one uses as the output of the device the output field orthogonally polarized to the input field, and at the same frequency, $A_-^{\text{out}} = tA_-$, one will have a zero output below threshold and a value rapidly growing with the input above threshold, which is the behavior that we need in our reshaping device. It is worthy to note that the present threshold $P_{\text{threshold}}^{\text{low}}$, equal to $T^2T_0/2g^2$ for small intensity transmission coefficients at both frequencies, Tt^2 and $T_0 = t_0^2$, is the threshold of a triply resonant OPO, which can be in the milliwatt range in optimized conditions.[6]

Two difficulties must be solved to operate this device. First, we have assumed perfect triple resonance to solve the equations. This is not an easy condition to fulfill, as the fields A_0, A_1, and A_2 see three different indices in the type II nonlinear crystal, corresponding to three different optical paths. As all the frequencies are fixed, we must then adjust precisely three parameters of the system to fulfill the triple-resonance conditions. Two parameters, the cavity length and the crystal temperature, are easily controllable, but a third one is needed. This last one could be the setting of a variable birefringent system in the cavity. We chose another approach, which is to insert a quarter-wave plate in the linear cavity, adjusted so that it induces a 90° rotation of the polarization plane for the fundamental wave when it is crossed twice by the beam inside the cavity and does not change the second-harmonic field polarization. In this configuration, for any crystal temperature, the eigenmodes of the cavity are automatically (A_+, A_-). We need then to adjust only two parameters to ensure the triple-resonance condition: the cavity length and the crystal temperature. Second, we have assumed a degenerate operation for the OPO. This is one possibility for the system. But a nondegenerate operation of the OPO can also take place, with signal and idler modes oscillating at different frequencies ω_1 and ω_2 such that $\omega_1 + \omega_2 = \omega_0$. This regime of cascading has been theoretically studied[7,8] and observed.[9] Actually, the system will oscillate in the regime (degenerate or nondegenerate) that has the lowest threshold. We will see in Subsection 4.A that one can find conditions for which it is indeed possible to observe the stable degenerate operation that is needed for reshaping without frequency change, which is necessary for practical applications. A forthcoming publication will give more precise insight into the operation of this kind of optical device

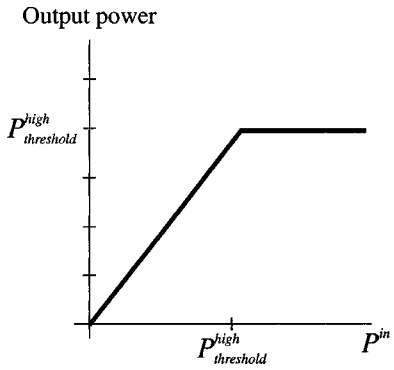

Fig. 2. Transmitted power I_{transm} by the second cavity as a function of the input pump power I_{in}.

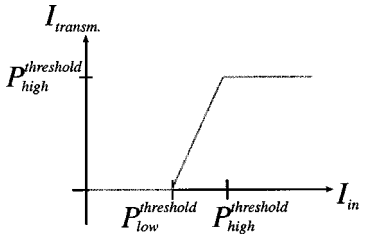

Fig. 3. Transmitted power through the total system as a function of the input pump power.

that contains, at the same time, second-order nonlinear elements and birefringent elements.

B. Second Optical System: Nondegenerate Optical Parametric Oscillator

The second system consists of a standard, nondegenerate, triply resonant OPO. It is well known that, in a laser above threshold, the gain is clamped to its threshold value by the condition that the saturated gain must equal the losses in the steady-state regime. The same behavior occurs in an OPO, as can be seen very easily from its steady-state equations, which are very similar to Eqs. (1)–(3), except that now the input power is put in the cavity on the high-frequency mode:

$$(1 - r_s)A_s = gA_pA_i^*, \tag{13}$$

$$(1 - r_i)A_i = gA_pA_s^*, \tag{14}$$

$$[1 - (r_p)^2]A_p = -gA_sA_i + t_pA_p^{\mathrm{in}}, \tag{15}$$

where A_s and A_i are the intracavity signal and idler mode amplitudes (these two modes oscillating at different frequencies); A_p is the intracavity pump amplitude; A_p^{in} is the input pump amplitude; and r_s, r_i, and r_p are the amplitude reflection coefficients of the coupling mirror at the signal, idler, and pump frequencies. For the pump field, one has assumed that the cavity has two identical coupling mirrors, of amplitude reflection and transmission coefficients r_p and t_p, one used as the input and the second as the output of our optical device.

Solving these very well-known equations,[3] one finds that there are two different regimes, depending on the pump intensity $P_{\mathrm{pump}} = |A_p^{\mathrm{in}}|^2$, separated by a threshold $P^{\mathrm{high}}_{\mathrm{threshold}}$ (see Fig. 2):

1. For $P_{\mathrm{pump}} < P^{\mathrm{high}}_{\mathrm{threshold}} = [t_p{}^2(1 - r_s)(1 - r_i)]/g^2$, one has $A_s = A_i = 0$. No parametric oscillation takes place. The OPO cavity is a pure passive, resonant, Fabry–Perot cavity with input and output mirrors of equal transmission. Its transmission is therefore 1, and the device is exactly transparent.

2. For $P_{\mathrm{pump}} > P^{\mathrm{high}}_{\mathrm{threshold}}$, one has $A_s \neq 0$ and $A_s \neq 0$, which occurs only when $|A_p|^2 = [(1 - r_s)(1 - r_i)]/g^2$, whatever the input pump field is: The intracavity pump power is therefore clamped to a value independent of the input, and the output pump field is then clamped to its value at threshold. The excess power brought by the pump is then transferred to the signal and idler beams.

Let us stress that here also the pump threshold $P_{\mathrm{threshold}}{}^{\mathrm{high}}$ is the threshold of a triply resonant OPO, which can be very low. But now the system is much simpler to operate than the previous one, as the frequencies of the signal and idler modes are not *a priori* given (except that their sum is equal to the pump frequency). There is one more degree of freedom than in the first device, and the cavity length and crystal temperature are the only two parameters that need to be adjusted to get the triply resonant condition.

C. Total System

If the two previously described devices are put in series, one obtains overall input–output characteristics that are sketched in Fig. 3. This curve is close to the one we need for pulse reshaping, except for the intermediate region $P^{\mathrm{low}}_{\mathrm{threshold}} < P_{\mathrm{pump}} < P^{\mathrm{high}}_{\mathrm{threshold}}$, for which the response is linear. The best reshaping will be obtained when this central part is as steep as possible.

3. EXPERIMENTAL SETUP

The input beam is produced by a Nd:YAG laser at 1.06 μm (Lightwave 126-1064-700). To produce a light pulse, we use an acousto-optic modulator to modulate the intensity of the transmitted beam (modulation frequency $\approx$3 kHz). To mimic the high-frequency noise existing on the pulse, we superimpose on the envelope a high-frequency modulation ($\approx$100 kHz) and simulate the high-frequency noise [Fig. 4(a)].

A. Intracavity Second-Harmonic Generation–Optical Parametric Oscillator

The characteristics of the two cavities are summarized in Table 1. The first cavity has highly reflecting mirrors for both 1.06 and 0.53 μm. The pump at 1.06 μm is sent at a 45° angle with respect to the crystal axis. The output beam is separated from the input by use of a polarizing beam splitter in front of the optical device. At low input power, it is first converted into green light by a standard doubling process. When the intracavity green power is sufficient, parametric downconversion occurs, which transfers the power back to the pump wavelength but on the orthogonal polarization. However, this system has a high threshold, above 600 mW in our experimental conditions. To reduce this threshold, we have added a quarter-wave plate at 1.06 μm inside the cavity. In that case, we observed a much more efficient intracavity second-harmonic generation, and a parametric oscillation threshold could be as low as 300 mW. This fairly large threshold is mainly due to the fact that the reflection coefficients

were not optimized (in particular, the green reflection coefficients should be maximum, which is not the case).

B. Nondegenerate Optical Parametric Oscillation

This system has been described extensively in a previous publication.[6,10] Let us briefly mention here its main features. A periodically poled lithium niobate (PPLN) crystal with an inversion period of 30 μm is placed inside a symmetric cavity that has a large finesse (over 200) for the wavelengths around 2 μm and a lower finesse at 1 μm (around 40). The crystal temperature is kept close to the degeneracy temperature (parametric conversion between 1.06 and 2.12 μm), so that parametric oscillation occurred for all cavity lengths within a pump resonance because of the overlap between the oscillation ranges of nearby signal and idler pairs of modes of wavelengths close to 2 μm.[6] The threshold was of the order of a few milliwatts. This threshold was chosen to obtain a transmitted field as close as possible to a square function: Its value is much lower than the maximum intensity at the output of the first cavity to ensure a steep transmission function. Let us also mention that in our experiment the input and output mirrors for the 1.06-μm beam were not of equal transmission. As a result, the power of the transmitted beam was very small compared with the input one and not equal, as in the theoretical approach of Section 2. This is due to the fact that we used, instead of an optimized cavity, an existing one as used in the experiment described in Ref 6.

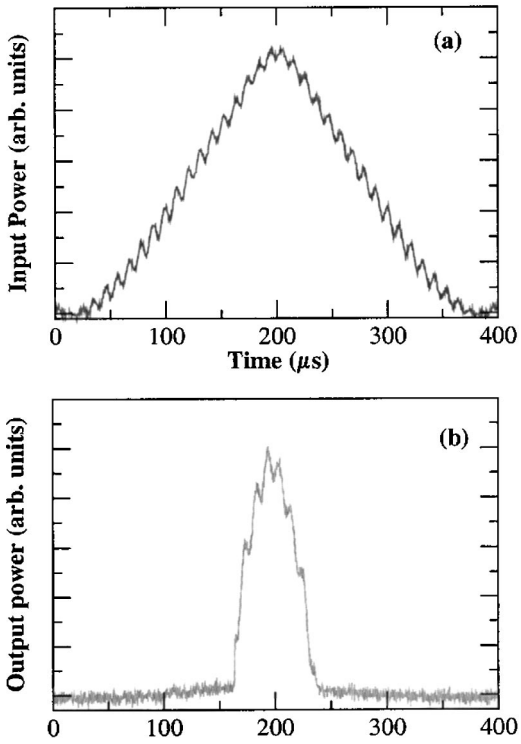

Fig. 4. Experimental results for cavity 1: (a) input power as a function of time and (b) output power as a function of time.

4. EXPERIMENTAL RESULTS

A. Intracavity Second-Harmonic Generation–Optical Parametric Oscillator

Figure 4 shows the input and output intensities of the first device as a function of time. The maximum input power on this cavity was 350 mW in order to be above the threshold $P_{\text{threshold}}^{\text{low}}$ mentioned above. It can be seen in Fig. 5 that the effect of the cavity is close to a perfect high-pass filter, as far as intensities are concerned: Powers below $P_{\text{threshold}}^{\text{low}}$ are not transmitted, whereas those above this value are linearly transmitted.

A crucial point of the device is that the output beam (orthogonally polarized reflected pump beam) is at the same frequency as the input beam. In a first experiment we looked at the interference pattern between the input and the output beams and observed that there were no fringes when the second-harmonic beam was not TEM_{00}. Clear fringes appeared only when, by a careful alignment and crystal temperature tuning, the green output was TEM_{00}. The frequency-degenerate operation was corroborated by a second experiment, in which we used a confocal Fabry–Perot cavity to monitor the frequency of the output beam, orthogonally polarized with respect to the input beam. The confocal Fabry–Perot cavity is formed by two curved mirrors with radius of 50 mm and reflectivity of 95% for 1.064 μm so that the free spectral range is 1.5 GHz. Figure 6 shows the output beam and the pump beam transmitted intensities through the confocal Fabry–Perot cavity when scanning the analysis cavity at 60 Hz and scanning the self-pumped OPO at 650 Hz. This figure shows that, when the system is not perfectly tuned up, it oscillates in a nondegenerate regime and generates sidebands around the pump frequency (Fig. 6, left), whereas one can find experimental conditions for which the down-converted output has the same frequency as the pump, within the experimental uncertainties (Fig. 6, right).

B. Nondegenerate Optical Parametric Oscillation

We have plotted in Fig. 7 the relevant intensities for the second cavity as a function of time: Figure 7(a) shows

Table 1. Characteristics of the Cavities[a]

			Input Mirror			End Mirror		
Cavity	Crystal	Cavity Length (mm)	R_c	R_λ (%)	$R_{2\lambda}$ (%)	R_c	R_λ (%)	$R_{2\lambda}$ (%)
1 $\lambda = 532$ nm	KTP	50	50	>99.9	95	50	90	>99.9
2 $\lambda = 1064$ nm	PPLN	65	30	87	99.8	30	99.8	99

[a] R_c radius of curvature in millimeters; $R_{(2)\lambda}$ reflection coefficient at (2)λ.

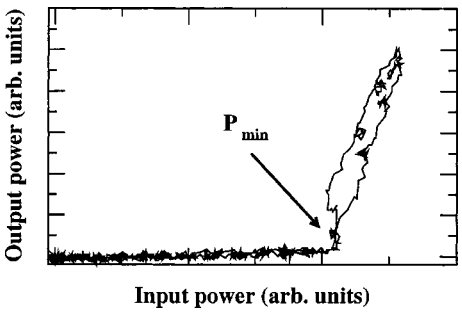

Fig. 5. Transfer function of the first cavity.

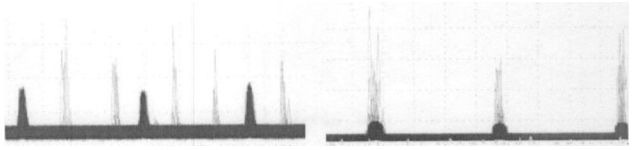

Fig. 6. Downconverted beam and pump beam transmitted intensities through the confocal Fabry–Perot cavity as a function of the confocal Fabry–Perot cavity length. The sharp and light peaks are the transmission of the downconverted output, and the blunt and dark peaks are the transmission of the pump beam. Left, the nondegenerate case; right, the degenerate case.

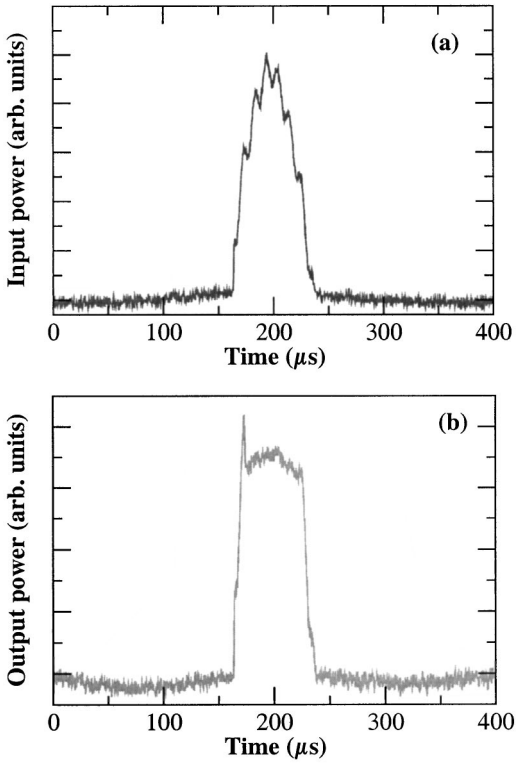

Fig. 7. Experimental results for cavity 1: (a) input power as a function of time and (b) output power as a function of time.

the incident intensity, and Fig. 7(b) shows the transmitted intensity. The output intensity displays a very clear clamping of the power above the threshold $P_{\text{threshold}}^{\text{high}}$, at a value equal to the transmitted pump power at threshold, typically a few milliwatts. In Fig. 8 the low-pass filter (for intensities) effect of this cavity is shown via its transfer function.

The peak that one observes at the beginning of the flat top of the transmitted intensity is due to a dynamical effect of delayed bifurcation that has already been observed in OPOs when their pump power is scanned with time.[11] As the incoming pump power increases above threshold, the onset of the oscillation is delayed by a time interval that is larger than the characteristic evolution times of the cavity.

C. Total Cascaded System

The complete experimental setup is shown in Fig. 9. The beam reflected by the intracavity second-harmonic generation–OPO is separated from the input beam by a polarizing beam splitter and sent to the nondegenerate OPO. The output beam intensity and the experimental transfer function for the total system are shown in Fig. 10. One observes that the time dependence of the output beam intensity is close to a rectangular pulse and, accordingly, that the transfer function shows the desired behavior with a response very close to a step function.

5. POSSIBLE IMPLEMENTATION TO VERY HIGH BIT RATES AT 1.5 μm

In all-optical pulse-reshaping systems, two parameters play an important role: the operating power and the re-

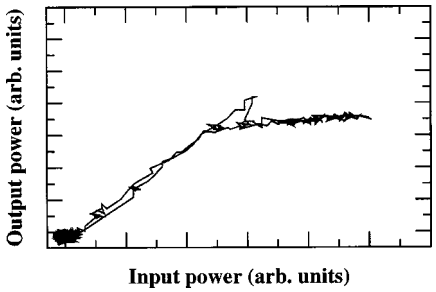

Fig. 8. Transfer function of the second cavity.

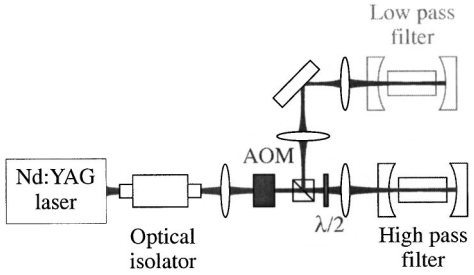

Fig. 9. Experimental setup with the two cavities in series showing the intracavity second-harmonic generation–OPO (low-pass filter) and nondegenerate OPO (high-pass filter).

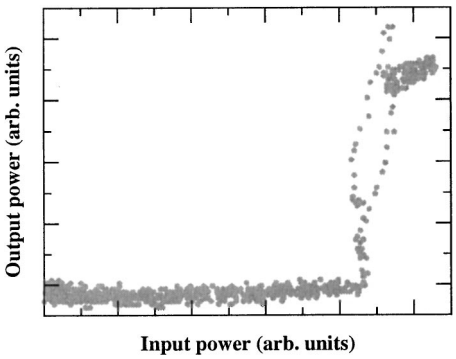

Fig. 10. Total transfer function of the system.

sponse time. In the present demonstration experiment, the incident power on the first cavity is approximately 350 mW, which is beyond the current powers of optical telecommunication pulses. This is mainly due to the fact that the first cavity is not optimized. Thresholds in the range of tens of milliwatts could be obtained by using high-quality materials and coatings and optimizing the cavity parameters. The response time of our present system is rather long, of the order of 200 ns: It is related to the cavity build-up time of the two cavities that are long cavities with rather high finesses. The most important question for the future of our proposed technique is whether our system can be modified and optimized to be able to reach very high bit rates, namely, 40 Gbit/s, and at the telecommunication wavelength of 1.5 μm. We will address this question in the present section.

Several nonlinear materials are compatible with the telecommunication wavelength, namely, gallium arsenide, aluminum gallium arsenide, or zinc selenide. These materials possess very large nonlinearities, as large as 120 pm/V in the case of gallium arsenide, but they cannot be phase matched by use of birefringence.

The rising time issue is the most difficult to solve. To reduce this time, one must use small cavities and therefore use shorter nonlinear crystals or lower reflectivities or both for the mirrors, two methods that have the detrimental effect of increasing the thresholds at the same time.

The threshold of a triply resonant OPO is given by

$$P_{\text{threshold}} = \frac{T_0 T_1 T_2}{64 \chi^2 {L_c}^2}, \tag{16}$$

where T_i denotes the transmission coefficient of the cavity for mode i, L_c is the crystal length, and χ is the nonlinear coupling strength depending on the nonlinearity, geometry, and optical indices through the relation

$$\chi = d_{\text{eff}} \frac{w_0 w_1 w_2}{{w_0}^2 {w_1}^2 + {w_0}^2 {w_2}^2 + {w_1}^2 {w_2}^2} \left(\frac{\hbar \omega_0 \omega_1 \omega_2}{\pi \epsilon_0 c^3 n_0 n_1 n_2} \right)^{1/2}, \tag{17}$$

where d_{eff} is the crystal nonlinearity in meters per volt. w_i is the waist size, ω_i is the pulsation, and n_i are the indices of refraction of the three interacting modes. Assuming that the system is operated close to frequency degeneracy, that is, $\omega_{1,2} = \omega_0/2$, and that the pump, signal, and idler indices and Rayleigh ranges are identical, the nonlinear coupling strength can be expressed in terms of wavelength and Rayleigh length as

$$\left(\frac{\chi_{\text{exp}}}{\chi} \right)^2 = \left[\frac{(d_{\text{eff}})_{\text{exp}}}{d_{\text{eff}}} \right]^2 \frac{z_R}{(z_R)_{\text{exp}}} \left[\frac{\lambda_0}{(\lambda_0)_{\text{exp}}} \right]^4 \left(\frac{n}{n_{\text{exp}}} \right)^2, \tag{18}$$

where the index exp denotes experimental values and λ_0, $(\lambda_0)_{\text{exp}}$ denote the pump wavelength in the vacuum; these two wavelengths are different because our experiment was performed with a $(\lambda_0)_{\text{exp}} = 532$-nm pump, whereas a telecom implementation would require $\lambda_0 \approx 1550$ nm.

If we also assume that the cavity length is equal to the crystal length, one can use the expression for the finesse as a function of the cavity rise time:

$$\mathcal{F} = \frac{\pi c \tau}{2 n L_c}. \tag{19}$$

We now obtain the following formula for the ratio of the thresholds:

$$\frac{P_{\text{threshold}}}{P_{\text{exp}}} = (\mathcal{F}_0 \mathcal{F}_1 \mathcal{F}_2)_{\text{exp}} \left(\frac{2n}{\pi c \tau} \right)^3 \left[\frac{(d_{\text{eff}})_{\text{exp}}}{d_{\text{eff}}} \right]^2 \frac{z_R}{(z_R)_{\text{exp}}} \times \left[\frac{\lambda_0}{(\lambda_0)_{\text{exp}}} \right]^4 \left(\frac{n}{n_{\text{exp}}} \right)^2 {L_{\text{exp}}}^2 L_c. \tag{20}$$

One obtains a counterintuitive result, namely, that the threshold becomes lower as the crystal/cavity length diminishes. This is due to the fact that the finesse is fixed by the value of the cavity length in order to keep the cavity lifetime τ constant. A small cavity is thus desirable to obtain a low threshold as well as a short rise time. The experimental values correspond to an optimized cavity containing a KTP crystal pumped by a frequency-doubled Nd:YAG laser at 532 nm generating signal and idler around 1064 nm, yielding $P_{\text{exp}} = 20$ mW with $n_{\text{exp}} \approx 1.8$, $(d_{\text{eff}})_{\text{exp}} = 3$ pm/V, $L_{\text{exp}} = 1$ cm, and $(\mathcal{F}_{0,1,2})_{\text{exp}} = 115$. When one sets a cavity/crystal length of 10 μm, a rise time τ of 10 ps (compatible with an operating bit rate of 40 Gbit/s), and a Rayleigh length of 10 μm compatible with the crystal length, one obtains a finesse $\mathcal{F} \approx 140$ and threshold $P_{\text{threshold}} \approx 110$ mW with the values corresponding to gallium arsenide ($n = 3.4$ and $d_{\text{eff}} = 120$ pm/V). This value of the threshold is compatible with the values used in optical telecommunications. The very short length of the crystal is also an advantage as one can have a crystal length equal to or shorter than the coherence length of the material, which partly removes the problem of phase matching. It is important to note that the variation of the threshold with τ is very fast so that a small increase of the rise time up to 15 ps leads to a similar threshold by use of lithium niobate ($n = 2.2$ and $d_{\text{eff}} = 20$ pm/V).

We have shown in this section that the realization of very short rise-time systems for all-optical reshaping is within reach by developing current techniques and using available materials. However, because of the presence of the resonance cavity, this system is able to reshape only optical pulses centered around a given wavelength.

6. CONCLUSION

We have demonstrated that optical cavities containing $\chi^{(2)}$ media can be used for all-optical passive reshaping of optical pulses. We have experimentally obtained reshaping with a threshold compatible with optical powers propagating in optical fibers. We have shown that very fast response times can be realized using very short monolithic cavities made of high nonlinearity crystals.

ACKNOWLEDGMENTS

Laboratoire Kastler Brossel, of the Ecole Normale Supérieure and the Université Pierre et Marie Curie, is associated with the Center National de la Recherche Scienti-

fique. This research was supported by France-Telecom (project CTI 98-9.003). The authors thank V. Berger for fruitful discussions.

T. Coudreau's e-mail address is coudreau @spectro.jussieu.fr.

*On leave from the Key Laboratory for Quantum Optics, Shanxi University, Taiyuan, China.

†Also with the Pôle Matériaux et Phénomènes Quantiques, FR, Centre National de la Recherche Scientifique 2437.

REFERENCES

1. J. Simon, L. Billes, A. Dupas, B. Kowalski, M. Henry, and B. Landousies, "All-optical regeneration," presented at the 24th European Conference on Optical Communications, Madrid, Spain, September 20–24, 1998.
2. J. Lucek and K. Smith, "All-optical signal regenerator," Opt. Lett. **18**, 1226–1228 (1993).
3. T. Debuisschert, A. Sizmann, E. Giacobino, and C. Fabre, "Type-II continuous-wave optical parametric oscillators: oscillation and frequency-tuning characteristics," J. Opt. Soc. Am. B **10**, 1668–1680 (1993).
4. Z. Y. Ou, "Quantum-nondemolition measurement and squeezing in type-II harmonic generation with triple resonance," Phys. Rev. A **49**, 4902–4911 (1994).
5. U. Peschel, C. Etrich, and F. Lederer, "Symmetry breaking and self-oscillations in intracavity vectorial second-harmonic generation," Opt. Lett. **23**, 500–502 (1998).
6. M. Martinelli, K. S. Zhang, T. Coudreau, A. Maître, and C. Fabre, "Ultra-low threshold CW triply resonant OPO in the near infrared using periodically poled lithium niobate," J. Opt. A, Pure Appl. Opt. **3**, 300–303 (2001).
7. S. Schiller, R. Bruckmeier, and A. White, "Classical and quantum properties of the subharmonic-pumped parametric oscillator," Opt. Commun. **138**, 158–171 (1997).
8. A. G. White, P. K. Lam, M. S. Taubman, M. A. M. Marte, S. Schiller, D. E. McClelland, and H. A. Bachor, "Classical and quantum signatures of competing $\chi^{(2)}$ nonlinearities," Phys. Rev. A **55**, 4511–4515 (1997).
9. K. Schneider and S. Schiller, "Multiple conversion and optical limiting in a subharmonic-pumped parametric oscillator," Opt. Lett. **6**, 363–365 (1997).
10. K. S. Zhang, T. Coudreau, M. Martinelli, A. Maître, and C. Fabre, "Generation of bright squeezed light at 1.06 μm using cascaded nonlinearities in a triply resonant cw periodically-poled lithium niobate optical parametric oscillator," Phys. Rev. A **64**, 033815, 1–6 (2001).
11. C. Richy, K. I. Petsas, E. Giacobino, C. Fabre, and L. Lugiato, "Observation of bistability and delayed bifurcation in a triply resonant optical parametric oscillator," J. Opt. Soc. Am. B **12**, 456–461 (1995).